

# Sum of Squares-Based Range Estimation of an Object Using a Single Camera via Scale Factor

Won-Hee Kim\*, Cheol-Joong Kim\*\*, Myunghwan Eom\*\*\* and Dongkyoung Chwa†

**Abstract** – This paper proposes a scale factor based range estimation method using a sum of squares (SOS) method. Many previous studies measured distance by using a camera, which usually required two cameras and a long computation time for image processing. To overcome these disadvantages, we propose a range estimation method for an object using a single moving camera. A SOS-based Luenberger observer is proposed to estimate the range on the basis of the Euclidean geometry of the object. By using a scale factor, the proposed method can realize a faster operation speed compared with the previous methods. The validity of the proposed method is verified through simulation results.

**Keywords:** Sum of squares, Range estimation, Scale factor, Camera

## 1. Introduction

Recently, studies on vision-based control theory have been actively employed in the vision-based control systems [1-4] and also promoted by the development of computer processor and camera technologies including stereo vision [5-8] and Kinect [9-11]. Stereo vision obtains distance information between the camera and the object using the distance information between two cameras. However, both stereo vision system and Kinect require either information of two cameras or a long computation time for image processing. Several methods have been studied in [12-14] to overcome these disadvantages. Since only two dimensional information can be obtained using a single camera, three dimensional information including the range should be recovered from the image of the camera. In the case of [13, 14], batch algorithms based on the algebraic equation relating the three dimensional and two dimensional information are studied. The motion of the object is, however, much restrictive and the real-time implementation of the batch algorithm using various images is very hard. With this problem in mind, the sum of squares (SOS)-based studies using a single camera [12] have been conducted to estimate the distance from the camera to the object. Still, when camera velocity is slow, it takes a long estimation time in the case of [12]. Therefore, we propose an SOS-based range estimation method using a scale factor, so as to realize a faster operation time and to simplify the required camera information unlike [8, 9]. Compared to [12], the proposed method has shorter estimation time by using a scale factor and a relaxed camera velocity assumption. Through simulations we

demonstrated the validity of the proposed method.

## 2. Camera Dynamics Modeling

When observing an object through a moving camera, the movement of feature points of the object is observed for every frame of video. Therefore, it requires the information of the relationship between the camera movement and feature points. Fig. 1 shows the camera and object coordinates.

Let  $F^*$  be the coordinate system of the camera at the initial time  $t_0$  (which corresponds to the initial point of the camera). Then, a camera frame  $F_C$  (which corresponds to the present position of the camera) changes through the rotation  $\bar{R}(t) \in SO(3)$  and translation  $\bar{x}_f \in \mathbb{R}^3$  from  $F^*$ . The feature point coordinates  $\bar{m}(t) \in \mathbb{R}^3$  are expressed in  $F_C$  as in (1) and its normalized coordinates  $m(t) \in \mathbb{R}^3$  as in (2).

$$\bar{m}(t) = [x_1(t) \ x_2(t) \ x_3(t)]^T \quad (1)$$

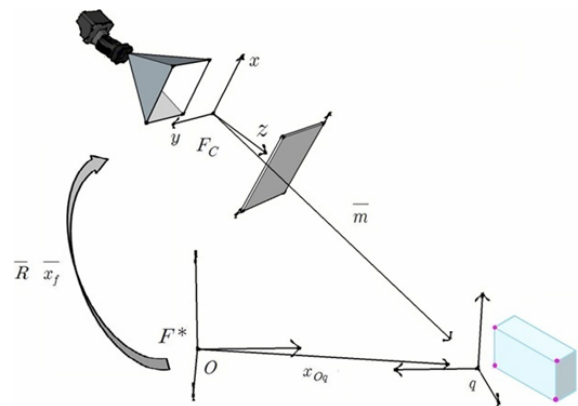


Fig. 1. The camera and object coordinates

† Corresponding Author: Dept. of Electrical and Computer Engineering, Ajou University, Korea. (dkchwa@ajou.ac.kr)

\* LG Chemk, Korea. (kwh808@ajou.ac.kr)

\*\* Hyundai Mobis, Korea. (cjoongkim@gmail.com)

\*\*\* Doosan Corporation Mottrol, Korea. (myunghwan.eom@gmail.com)

Received: July 24, 2016; Accepted: May 10, 2017

$$m(t) = \begin{bmatrix} \frac{x_1(t)}{x_3(t)} & \frac{x_2(t)}{x_3(t)} & 1 \end{bmatrix}^T. \quad (2)$$

For the derivation of the dynamics for the range estimation, the state  $y(t)$  needs to be introduced based on (1) or (2) instead of directly using the coordinates in (1) or (2) as follows:

$$y(t) := [y_1(t) \ y_2(t) \ y_3(t)]^T = \begin{bmatrix} \frac{x_1(t)}{x_3(t)} & \frac{x_2(t)}{x_3(t)} & \frac{1}{x_3(t)} \end{bmatrix}^T. \quad (3)$$

The normalized coordinates  $m(t)$  and the pixel coordinates satisfy the relationship

$$p = A_C m \quad (4)$$

where  $p(t) = [u, v, 1]^T$  can be obtained by the coordinates of the feature point  $u(t), v(t) \in \mathbb{R}$ , and  $A_C \in \mathbb{R}^{3 \times 3}$  is determined by camera calibration. As in (4),  $m(t)$  is gained from  $p(t)$  and  $A_C$ . It can provide the first two components of  $y(t)$ . On the other hand,  $y_3(t)$  is the inverse of the range  $x_3(t)$  and thus its estimate can be used to obtain the range estimate.

Object point  $q$  is represented in the camera frame  $F_C$  as

$$\bar{m}(t) = \bar{x}_f + \bar{R}x_{Oq} \quad (5)$$

where  $x_{Oq}$  is a vector starting from the origin of  $F^*$  to  $q$  in  $F_C$ . The time derivative of the variable in (5) can be represented as follows:

$$\dot{\bar{m}}(t) = [\omega]_X \bar{m} + v_r. \quad (6)$$

Here,  $[\omega]_X \in \mathbb{R}^{3 \times 3}$  is skew-symmetric with the camera angular velocity  $\omega(t) = [\omega_1 \ \omega_2 \ \omega_3]^T \in \mathbb{R}^3$ , and  $v_r(t)$  is the relative velocity between the camera and the point

$$v_r = v_c - \bar{R}\bar{v}_p. \quad (7)$$

Here,  $v_c(t) = [v_{cx} \ v_{cy} \ v_{cz}]^T \in V_c \subset \mathbb{R}^3$  is the camera velocity,

$\bar{R}\bar{v}_p := v_p(t) = [v_{px} \ v_{py} \ v_{pz}]^T \in V_p \subset \mathbb{R}^3$  is a velocity of the point  $q$  represented in frame  $F_C$ , and  $\bar{v}_p(t) = [\bar{v}_{px} \ \bar{v}_{py} \ \bar{v}_{pz}]^T \in \bar{V}_p \subset \mathbb{R}^3$  is a velocity of  $q$  represented in  $F^*$ .

Using (3) and (6), the dynamics of  $y(t)$  can be represented as

$$\begin{cases} \dot{y}_1 = (v_{cx} - y_1 v_{cz})y_3 - y_1 y_2 \omega_1 + (1 + y_1^2)\omega_2 \\ \quad - y_2 \omega_3 - (v_{px} - y_1 v_{pz})y_3 \\ \dot{y}_2 = (v_{cy} - y_2 v_{cz})y_3 - (1 + y_2^2)\omega_1 + y_1 y_2 \omega_2 \\ \quad + y_1 \omega_3 - (v_{py} - y_2 v_{pz})y_3 \\ \dot{y}_3 = -y_3^2 v_{cz} - y_2 y_3 \omega_1 + y_1 y_3 \omega_2 + y_3^2 v_{pz}. \end{cases} \quad (8)$$

Here, the states  $y_1(t)$  and  $y_2(t)$  are available from (4). On the other hand,  $y_3(t)$  is unmeasurable and thus should be estimated.

### 3. Design of Range Observer

The motion dynamics in (8) are represented using polynomials with static object (i.e.,  $v_p = 0$ ) as follows:

$$\begin{bmatrix} \dot{y}_1 \\ \dot{y}_2 \\ \dot{y}_3 \end{bmatrix} = \begin{bmatrix} \omega_2 y_1 & -\omega_3 - \omega_1 y_1 & v_{cx} - y_1 v_{cz} \\ \omega_3 + \omega_2 y_2 & \omega_1 y_2 & v_{cy} - y_2 v_{cz} \\ \omega_2 y_3 & -\omega_1 y_3 & -y_3 v_{cz} \end{bmatrix} \begin{bmatrix} y_1 \\ y_2 \\ y_3 \end{bmatrix} + \begin{bmatrix} \omega_2 \\ -\omega_1 \\ 0 \end{bmatrix}. \quad (9)$$

By the camera velocity assumption such as  $v_{cz} = 0$ , the motion dynamics become

$$\dot{y} = Ay + \alpha \quad (10)$$

where

$$A = \begin{bmatrix} \omega_2 y_1 & -\omega_3 - \omega_1 y_1 & v_{cx} \\ \omega_3 + \omega_2 y_2 & \omega_1 y_2 & v_{cy} \\ \omega_2 y_3 & -\omega_1 y_3 & 0 \end{bmatrix}, \quad \alpha = \begin{bmatrix} \omega_2 \\ -\omega_1 \\ 0 \end{bmatrix}.$$

The SOS-based observer for the estimation of  $y_3$  is designed as follows:

$$\begin{cases} \dot{\hat{y}} = A\hat{y} + L(z - \hat{z}) + \alpha \\ z = C\hat{y}. \end{cases} \quad (11)$$

where  $C = \begin{bmatrix} 1 & 0 & 0 \\ 0 & 1 & 0 \end{bmatrix}$  is an output matrix. Using the range observer in (11), the error dynamics become

$$\dot{e} = \tilde{A}e + \zeta - LCe \quad (12)$$

where

$$e = y - \hat{y}, \quad \tilde{A} = \begin{bmatrix} \omega_2 (y_1 + \hat{y}_1) & -\omega_3 & v_{cx} \\ \omega_3 & \omega_1 (y_2 + \hat{y}_2) & v_{cy} \\ 0 & 0 & 0 \end{bmatrix}, \text{ and}$$

$$\zeta = \begin{bmatrix} -\omega_1 (y_1 y_2 - \hat{y}_1 \hat{y}_2) \\ \omega_2 (y_1 y_2 - \hat{y}_1 \hat{y}_2) \\ \omega_2 (y_1 y_3 - \hat{y}_1 \hat{y}_3) + \omega_1 (y_2 y_3 - \hat{y}_2 \hat{y}_3) \end{bmatrix}.$$

The observer gain  $L$  should be designed to achieve the stabilization of the error dynamics in (12), which results in the design of a range observer. Unlike the previous method

[12], where  $\omega_1$ ,  $\omega_2$  should be zero, the proposed method eliminates the camera velocity assumption by using Lemma 1.

**Lemma 1:** Given matrices  $D(x)$ ,  $E(x)$ , and  $S(x) = S^T(x)$  of appropriate dimensions, suppose that the following inequality holds:

$$S(x) + D(x)F(x)E(x) + E^T(x)F^T(x)D^T(x) < 0 \quad (13)$$

where  $F(x)$  satisfies  $F^T(x)F(x) \leq I$ . Then, for some  $\varepsilon > 0$ , the following inequality should hold:

$$S(x) + \begin{bmatrix} \varepsilon D(x) & \varepsilon^{-1} E^T(x) \end{bmatrix} \begin{bmatrix} D^T(x) \\ E(x) \end{bmatrix} < 0. \quad (14)$$

**Proof:**  $\{\varepsilon^{1/2}D(x) - \varepsilon^{-1/2}E(x)\}^T \{\varepsilon^{1/2}D(x) - \varepsilon^{-1/2}E(x)\} \geq 0$  can be used to derive

$$E^T(x)D(x) + D^T(x)E(x) \leq \varepsilon D^T(x)D(x) + \varepsilon^{-1}E^T(x)E(x).$$

Next,  $\{F(x)D(x) - E(x)\}^T \{F(x)D(x) - E(x)\} \geq 0$  can be used to derive

$$E^T(x)F(x)D(x) + D^T(x)F^T(x)E(x) \leq E^T(x)D(x) + D^T(x)E(x)$$

Thus, (14) follows from these inequalities. (Q.E.D.)

Also,  $\zeta$  satisfies the following norm-bounded conditions:

$$F_1^T F_1 < I, \quad F_2^T F_2 < I \quad (15)$$

where

$$D_1 = \text{diag}(-\omega_1, \omega_2, \omega_2)$$

$$D_2 = \text{diag}(0, 0, \omega_1)$$

$$F_1 = \text{diag}(y_1 y_2 - \hat{y}_1 \hat{y}_2, y_1 y_2 - \hat{y}_1 \hat{y}_2, y_1 y_3 - \hat{y}_1 \hat{y}_3)$$

$$F_2 = \text{diag}(0, 0, y_2 y_3 - \hat{y}_2 \hat{y}_3)$$

$$E_1 = E_2 = I.$$

Let  $\bar{A} = \frac{1}{d_s} \tilde{A}$  and  $\bar{L} = \frac{1}{d_s} L$ , where  $0 < d_s \leq 1$  is a

constant scale factor introduced to have the quick estimation performance. Then, instead of the error dynamics in (12), the modified error dynamics given by

$$\dot{\bar{e}} = \bar{A}\bar{e} + \zeta - \bar{L}C\bar{e} \quad (16)$$

are used. It should be noted here that when  $d_s$  is chosen to be small,  $\bar{e}$  converges to its steady state value very quickly. Thus, the modified error dynamics in (16) can be used to obtain the range estimate by considering that the relationship between the steady state value of  $e$  and that

of  $\bar{e}$  exists. The observer gain  $\bar{L}$  which is needed for the design of the range observer can be designed as in the following theorem.

**Theorem 1:** Suppose that the error dynamics are given by (16) and the conditions in (17) and (18) are satisfied for a symmetric  $X$  and a polynomial matrix  $M$ .

$$v^T (X - \varepsilon_1 I) v \text{ is SOS} \quad (17)$$

$$-v^T (\alpha + \beta) v \text{ is SOS} \quad (18)$$

where  $\varepsilon_1, \varepsilon_2, \varepsilon_3 > 0$  are constants,  $\alpha = \bar{A}^T X + X\bar{A} - C^T M^T - MC$ ,  $\beta = \varepsilon_2 D_1^T D_1 + \varepsilon_2^{-1} E_1 E_1^T + \varepsilon_3 D_2^T D_2 + \varepsilon_3^{-1} E_2 E_2^T$ , and  $v \in \mathbb{R}^N$  is independent of  $e$ . A SOS-based observer gain  $\bar{L}$  can then be obtained by SOSTOOL [15] as

$$\bar{L} = X^{-1}M. \quad (19)$$

**Proof:** Since solutions  $X$  and  $M$  for the conditions in (17) and (18) exist, we can choose a Lyapunov function candidate  $V$  as

$$V = e^T X e \quad (20)$$

where  $X > 0$ . Its time derivative can then be arranged as

$$\begin{aligned} \frac{dV}{dt} &= \dot{e}^T X e + e^T X \dot{e} \\ &= \{\bar{A}e + \zeta - \bar{L}Ce\}^T X e + e^T X \{\bar{A}e + \zeta - \bar{L}Ce\} \\ &= e^T (\bar{A}^T X - C^T \bar{L}^T X) e + e^T (X\bar{A} - X\bar{L}C) e \\ &\quad + \zeta^T X e + e^T X \zeta \\ &\leq e^T (\gamma) e \end{aligned} \quad (21)$$

where

$$\gamma = \bar{A}^T X + X\bar{A} - C^T \bar{L}^T X - X\bar{L}C + E_1^T F_1^T D_1^T X + X D_2 F_2 E_2$$

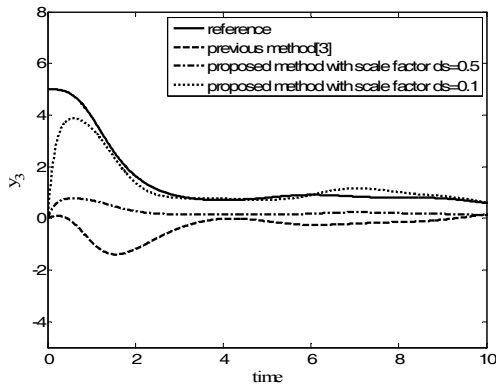
is negative definite and thus the time derivative in (21) is negative semi-definite by defining  $M = X\bar{L}$  and by using Lemma 1. In this way, the conditions of Theorem 1 in (17) and (18) can be obtained. (Q.E.D.)

## 4. Simulation Results

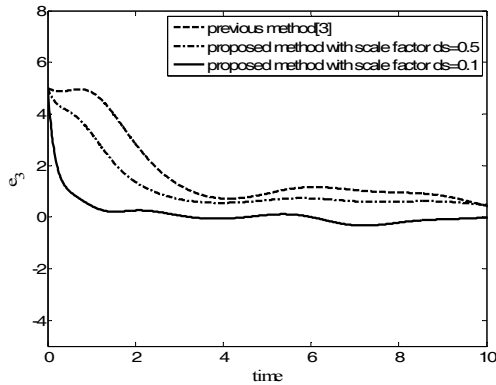
In this section, the validity of the proposed method will be verified through simulations. Two scenarios are shown in Table 1, where the velocities of the camera are set to be different. The first scenario is used for the comparison of the proposed method and the previous method [12] and the components of the camera linear velocity vector are time-varying. The second scenario is used for the comparison of the proposed method using a scale factor and the proposed method without a scale factor. In both scenarios, the scale

**Table 1.** Scenarios for the simulation

scenario	$v_c(t)(m/s)$	$\omega_c(t)(rad/s)$
I	$v_{cx}(t) = 1 + 0.5\sin\left(\frac{\pi t}{8}\right)$	$\omega_1(t) = 0.1\sin\left(\frac{\pi t}{4}\right)$
	$v_{cy}(t) = 1 + 0.5\sin\left(\frac{\pi t}{4}\right)$	$\omega_2(t) = 0.1\sin\left(\frac{\pi t}{4}\right)$
	$v_{cz}(t) = 0$	$\omega_3(t) = 0.8$
II	$v_{cx}(t) = 0.5$	$\omega_1(t) = 0$
	$v_{cy}(t) = 0.5$	$\omega_2(t) = 0$
	$v_{cz}(t) = 0$	$\omega_3(t) = 0.5$



(a) Estimate of  $y_3$  in scenario I

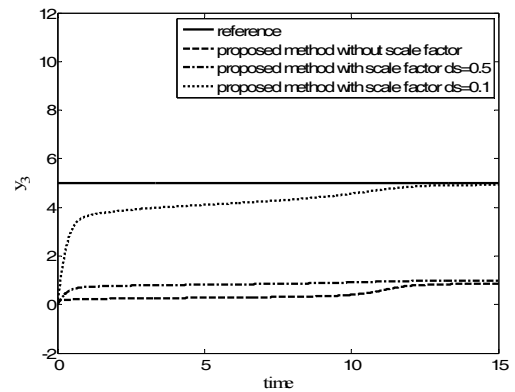


(b) Estimation error  $e_3$  in scenario I

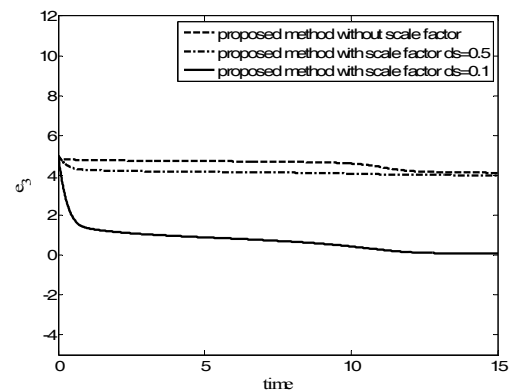
**Fig. 2.** Comparison of the range estimation performance of the proposed methods with the previous method

is set to be  $d_s = 0.1$  and the initial state is set to be  $y(0) = [5 \ 5 \ 5]^T$ . The value of  $d_s$  is chosen to be less than 1 in order to improve the transient estimation performance. The case when  $d_s = 1$  corresponds to the one without using the scale factor. Whereas the estimation speed in Figs. 2 and 3 was still slow in the case of  $d_s = 0.5$ ,  $d_s = 0.1$  results in the faster estimation response.

Fig. 2 shows that the range estimation performance of the proposed method is more satisfactory than the previous method [12] in that the range estimate quickly converge to the actual value as in Fig. 2(a). To see this more clearly, the



(a) Estimate of  $y_3$  in scenario II



(b) Estimation error  $e_3$  in scenario II

**Fig. 3.** Comparison of the range estimation performance of the proposed methods without and with the scale factor

estimation error is provided in Fig. 2(b). As mentioned before, the camera linear velocity is time-varying in this scenario and the estimation performance is guaranteed even for the time varying range.

Next, the validity of the introduction of the scale factor is shown in Fig. 3. Although the SOS-based range observer in (11) can work for the non-zero  $\omega_1$  and  $\omega_2$  and thus the constraints on the camera motion can be much relieved, the speed of the range estimation is also important. Therefore, we need to introduce the scale factor to improve the speed of the estimation performance. Whereas the results of the proposed method without scale factor is much slow in the case of scenario 2, the proposed method with scale factor results in much faster estimation performance in Fig. 3. All of the results in Figs. 2 and 3 show that the proposed method with a scale factor is better than both the previous method [12] and the proposed method without a scale factor.

### 5. Conclusion

We have proposed an SOS-based range estimation

method of an object using a moving single camera via a scale factor and verified its validity through simulations. Many previous methods have usually used multiple cameras. Even when a single camera is used, the camera motion should be much constrained and thus the estimation performance does not become satisfactory. To solve these limitations, SOS-based range estimation via a scale factor is proposed to design a range estimator. SOS method can use the polynomial form of nonlinear dynamics and the scale factor can increase the estimation speed so that the overall range estimation performance becomes satisfactory irrespective of the speed of the camera motion, unlike previous studies. The issues on the motion estimation of a moving object and the further relaxation of the constraint of the camera velocity can be pursued as a valuable future work.

### Acknowledgements

This work was supported by the National Research Foundation of Korea under a grant supported by the Korea government (MSIP) (2014R1A2A1A11053153) and by Basic Science Research Program through the National Research Foundation of Korea(NRF) funded by the Ministry of Science, ICT & Future Planning (2017 R1A2B4009486).

### References

- [1] J.-G. Kim and D. Lee, "Body Segmentation using Gradient Background and Intra-Frame Collision Responses for Markerless Camera-Based Games," *Journal of Electrical Engineering & Technology*, vol. 11, no. 1, pp. 234-240, Jan. 2016.
- [2] D. D. Pham, Q. K. Dang, and Y. S. Suh, "Golf Green Slope Estimation Using a Cross Laser Structured Light System and an Accelerometer," *Journal of Electrical Engineering & Technology*, vol. 11, no. 2, pp. 508-518, Mar. 2016.
- [3] S. Yun, B. Lee, Y.-J. Kim, Y. J. Lee, and S. Sung, "Augmented Feature Point Initialization Method for Vision/Lidar Aided 6-DoF Bearing-Only Inertial SLAM," *Journal of Electrical Engineering & Technology*, vol. 11, no. 6, pp. 1846-1856, Nov. 2016.
- [4] S.-W. Seo, G.-C. Lee, and J.-S. Yoo, "Motion Field Estimation Using U-Disparity Map in Vehicle Environment," *Journal of Electrical Engineering & Technology*, vol. 12, no. 1, pp. 428-435, Jan. 2017.
- [5] Y. Yakimovsky and R. Cunningham, "A System for extracting three-dimensional measurements from a stereo pair of TV cameras," *Computer Graphics and Image Processing*, vol. 7, no. 2, pp. 195-210, Apr. 1978.
- [6] W. Eric and L. Grimson, "Computational experiments with a feature based stereo algorithm," *IEEE*

- Transactions on Pattern Analysis and Machine Intelligence*, vol. PAMI-7, no. 1, pp. 17-33, Jan. 1985.
- [7] U. R. Dhond and J. K. Aggarwal, "Structure from stereo—a review," *IEEE Transactions on System, Man and Cybernetics*, vol. 19, no. 6, pp. 1489-1510, Nov. 1998.
- [8] J. Chiang, C. Hsia, H. Hsu, "A Stereo Vision-Based Self-Localization System," *IEEE Sensors*, vol. 13, no. 5, pp. 1677-1689, 2013.
- [9] M. Camplani, T. Mantecon, L. Salgado, "Depth-Color Fusion Strategy for 3-D Scene Modeling With Kinect," *IEEE Trans. Cybernetics*, vol. 43, no. 6, pp. 1560-1571, 2013.
- [10] S. Shen, N. Michael, and V. Kumar, "Autonomous Indoor 3D Exploration with a Micro-Aerial Vehicle," *Proceedings of IEEE International Conference on Robotics and Automation, Saint Paul, MN*, pp. 9-15, May. 2012.
- [11] S. Shen, N. Michael, and V. Kumar, "Autonomous Multi-Floor Indoor Navigation with a Computationally Constrained MAV," *Proceedings of IEEE International Conference on Robotics and Automation, Shanghai, China*, pp. 20-25, May. 2011.
- [12] C. Kim, D. Chwa, "Sum of Squares based Range Estimation for Camera Systems." Lecture Notes in Computer Science (including subseries Lecture Notes in Artificial Intelligence and Lecture Notes in Bioinformatics), 2013, 8102 LNAI(PART 1), pp. 668-678.
- [13] J. Kaminski and M. Teicher, "A general framework for trajectory triangulation," *Journal of Mathematical Imaging and Vision*, vol. 21, no. 1, pp. 27-41, Jul. 2004.
- [14] C. Yuan and G. Medioni, "3D reconstruction of background and objects moving on ground plane viewed from a moving camera," *IEEE Computer Society Conference on Computer Vision and Pattern Recognition, New York*, vol. 2, pp. 2261-2268, Jun. 2006.
- [15] SOSTOOLS Research: 'SOSTOOLS: Sum of Squares Optimization Toolbox for Matlab, version 3', <http://www.cds.caltech.edu/sostools>, accessed March 2014.



**Won-Hee Kim** received the B.S., M.S. degrees in electrical and computer engineering from Ajou University, Suwon, Korea, in 2014 and 2016, respectively. He is currently with LG Chem. His research interests include nonlinear control and disturbance observer theories and their applications to cyber physical systems (CPS) and vision-based control systems.



**Cheol-Joong Kim** received the B.S., M.S., and Ph.D. degrees in electrical and computer engineering from Ajou University, Suwon, Korea, in 2008, 2010, and 2014, respectively. He is currently with Hyundai Mobis. His research interests are nonlinear system, robust and fuzzy control theories with numerical analysis and their applications to the robotics; underactuated systems, including wheeled mobile robots and cranes; camera systems; and chaotic system and complex network.



**Myunghwan Eom** received the B.S., M.S., and Ph.D. degrees in electrical and computer engineering from Ajou University, Suwon, Korea, in 2009, 2011, and 2016, respectively. He is currently with Doosan Corporation Mottrol. His research interests include adaptive and robust nonlinear control theories and disturbance observer theories and their applications to robotics and underactuated mechanical systems, including pendubot, cranes, and autonomous unmanned vehicles.



**Dongkyoung Chwa** received the B.S. and M.S. degrees in control and instrumentation engineering and the Ph.D. degree in electrical and computer engineering from Seoul National University, Seoul, Korea, in 1995, 1997, and 2001, respectively. From 2001 to 2003, he was a Postdoctoral Researcher with Seoul National University, where he was also a BK21 Assistant Professor in 2004. Since 2005, he has been with the Department of Electrical and Computer Engineering, Ajou University, Suwon, Korea, where he is currently a Professor. He was a Visiting Scholar with the University of New South Wales at the Australian Defence Force Academy and the University of Melbourne, Melbourne, Vic., Australia, in 2003 and the University of Florida, Gainesville, in 2011. His research interests include nonlinear, robust, and adaptive control theories and their applications to robotics; underactuated systems, including wheeled mobile robots; underactuated ships; cranes; and guidance and control of flight systems.